Accepted Manuscript

Semi-hard magnetic properties of nanoparticles of cobalt ferrite synthesized by the co-precipitation process

N. Hosni, Karim Zehani, T. Bartoli, L. Bessais, H. Maghraoui-Meherzi

PII: S0925-8388(16)33015-8

DOI: 10.1016/j.jallcom.2016.09.252

Reference: JALCOM 39086

To appear in: *Journal of Alloys and Compounds*

Received Date: 24 June 2016

Revised Date: 8 September 2016

Accepted Date: 23 September 2016

Please cite this article as: N. Hosni, K. Zehani, T. Bartoli, L. Bessais, H. Maghraoui-Meherzi, Semi-hard magnetic properties of nanoparticles of cobalt ferrite synthesized by the co-precipitation process, *Journal of Alloys and Compounds* (2016), doi: 10.1016/j.jallcom.2016.09.252.

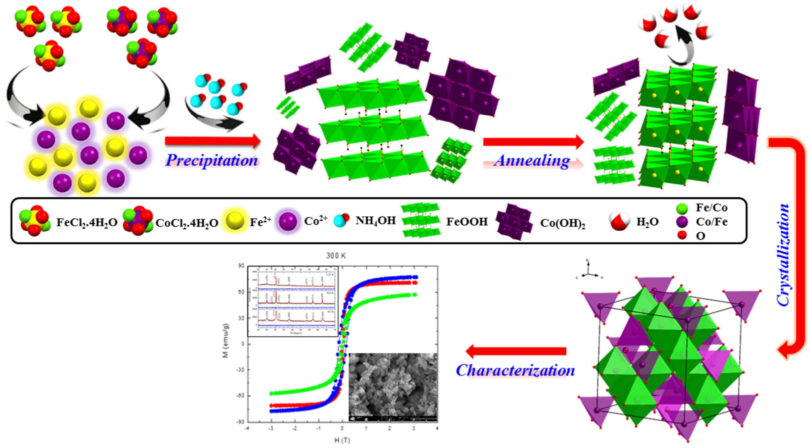
Precipitation
Annealing
Crystallization
Characterization
FeCl$_2$.4H$_2$O
CoCl$_2$.4H$_2$O
Fe^{2+}
Co^{2+}
NH$_4$OH
FeOOH
Co(OH)$_2$
H$_2$O
Fe/Co
Co/Fe
O
300 K
M (emu/g)
H (T)

Semi-hard magnetic properties of nanoparticles of cobalt ferrite synthesized by the co-precipitation process

N. Hosni[a], Karim Zehani[b,*], T.Bartoli[b], L. Bessais[b], H. Maghraoui-Meherzi[a]

[a] *Université de Tunis El-Manar, Faculté des Sciences de Tunis, Laboratoire de Chimie Analytique et Electrochimie, 2092 Tunis, Tunisie, LR99ES15.*
[b] *CMTR, ICMPE, UMR7182, CNRS Université Paris Est Créteil, 2-8 rue Henri Dunant, F-94320 Thiais, France.*

Abstract

The nanoparticles ferromagnetic materials $CoFe_2O_4$ have been synthesized by the co-precipitation method and annealed at various temperatures from 773 to 1223 K. The influence of the heat treatment on the structural, morphological and magnetic properties of $CoFe_2O_4$ nanoparticles was investigated. The structure, morphology and magnetic properties of the annealing samples were reached by mean of X-ray diffraction (XRD), scanning electron microscopy (SEM) techniques and measurement of hysteresis loop. The average crystallite size, lattice parameter and X-ray density were calculated from X-ray diffraction data. All samples have the cubic spinel structure with average crystallite sizes increasing from 30 to 178 nm with the temperature. The results show that $CoFe_2O_4$ nanoparticles prepared by this method have small and more uniform size. The measurements of the hysteresis loop, performed at both 10 K and 300 K, indicate a ferromagnetic behavior of nanoparticles. Also the measurement at 300 K shows that the sample annealed at 1023 K is magnetically harder than the other samples. The coercive fields are 1.58 kOe against the values inferior at 0.61 kOe for the other samples. Indeed, the remanent magnetization is 31.85 $emu.g^{-1}$ for the hard magnetic sample against 13.02 and 17.29 $emu.g^{-1}$ for the soft magnetic samples annealed at 773 and 1223 K, respectively. The origin of

*Corresponding author
Email address: zehani@icmpe.cnrs.fr (Karim Zehani)

the hard-soft magnetic properties of nanoparticles $CoFe_2O_4$ is discussed in terms of the co-existence of secondary phases β-Fe_2O_3, CoO_2 and the distribution of Fe^{2+} and Co^{2+} ions within the lattice.

Keywords: Nanoparticles; $CoFe_2O_4$; β-Fe_2O_3; Magnetic properties; Rietveld refinement.

1. Introduction

Recently, the synthesis of magnetic nanoparticles of spinel ferrites has been a field of intense study, owing to their optical, electronic and magnetic properties with high chemical and thermal stabilities. These materials are technologically important and have been used in many applications, including magnetic recording media and magnetic fluids for the storage and retrieval of information, magnetic resonance imaging (MRI) enhancement, catalysis, magnetically guided drug delivery, sensors and pigments [1, 2, 3]. Moreover nanoparticles spinel ferrites emerged as an important subclass of magnetic materials with attractive features (magnetic and electrical proprieties) and an increasing synthetic accessibility.

These ferrites belonging to AB_2O_4 group (family) are mainly controlled by the divalent cations, which occupy the tetrahedral A sites and the trivalent cation, which has a high degree of affinity for octahedral B sites. Cobalt ferrite particle material has an inverse spinel structure [4, 5]. The presence of the two transition metal ions at one crystallographic site leads to a unique type of hopping conductivity and magnetic coupling. Cobalt ferrite ($CoFe_2O_4$) is an interesting material because of its high magnetocrystalline anisotropy and its high coercivity and moderate magnetization [6, 7, 8]. These properties, along with their great physical and chemical stability, make $CoFe_2O_4$ nanoparticles suitable for magnetic recording applications such as audio and videotape and high-density digital recording disks and recent investigations have shown that the cobalt ferrite nanoparticles have photomagnetic properties [9, 10].

On the other hand, the spinel ferrites are synthesized by various techniques such as sol-gel [11], hydrothermal [12], ultrasonically assisted hydrothermal processes [13], reverse mi-celle synthesis [14], citrate precursor techniques [15, 16], electrochemical synthesis [17], combustion methods [18], solid-state reaction [19], and mechanical alloying [20, 21, 22], among them the co-precipitation shows a great promise as an effective synthetic approach. Widely used it allows a good control of the shape and the grain size distribution during the synthesis and stoichiometric composition of nanoparticles, not only for these reasons but also due to its economical perspectives. This work highlights the co-precipitation route to synthesize $CoFe_2O_4$ nanoparticles. The nanoparticles spinel ferrites were characterized by various analytical techniques to investigate the structural and the morphological properties of the nanoparticles. A spinel emphasis is put on the magnetic properties of such particles which have not been widely studied.

2. Experimental

All the chemical precursors were purchased from Aldrich and used without further purification. A series of nanoparticles ferrites with composition $CoFe_2O_4$ are synthesized by co-precipitation method using stoichiometric ratio of Co/Fe equal 1:2. The amount of salt solutions of 0.23M iron chloride ($FeCl_2.4H_2O$) and 0.16M of cobalt chloride ($CoCl_2.4H_2O$) were prepared. The solutions of appropriate concentrations are dissolved in de-ionized water and heated to 313 K under constant stirring for 180 min and in maintaining the $pH = 9-11$ by the addition of ammonium hydroxide (28%) NH_4OH solution. The co-precipitated products were then washed several times with de-ionized water. The precipitates were then filtered and dried overnight in the oven at 323 K to remove the water content. Finally, the precipitates of the product were ground to fine powder and then annealed at 773 , 973, 1023, 1073 and 1223 K in an electric furnace in air atmosphere for 6 h to obtain the spinel phase. The sample was slowly cooled down at 38 K/h, 63K/h, 70 K/h, 80K/h and 105 K/h respectively for 773 , 973, 1023, 1073 and 1223 K during 6 h and finally quenched to room temperature.

To investigate the structure of the synthesized nanoparticles, the structural characterization was performed by the powder X-ray diffraction using the BRUKER diffractometer with Cu-K$_\alpha$ target (λ = 1.5406 Å) to determine the crystallographic structure and identify the present phases. Scans of 2 h between 20° and 70° with $\Delta\theta = 0.02°$ steps and counting times of 22 s per point were measured at room temperature. The XRD data were refined using Rietveld method as implemented in the FullProf computer code [23, 24]. The magnetic measurements of the samples were carried out using a Physical Properties Measurement System (PPMS9 Quantum Design) under an applied field up to 3 T.

3. Results and discussion

3.1. Mechanism of formation of cobalt ferrite.

In co-precipitation method the formation of $CoFe_2O_4$ nanoparticles is observed when the ionic product of anion and cation exceeds the solubility product of metal oxide when the solution is saturated. The mechanism of reactions can be represented by following equations:

$$CoCl_2 + 2NH_4OH \longrightarrow Co(OH)_2 + 2NH_4Cl \tag{1}$$

$$8FeCl_2 + 14NH_4OH \longrightarrow 7Fe(OH)_2 + 14NH_4Cl + Fe^{2+} + 2Cl^- \tag{2}$$

The mechanism for oxidation of ferrous hydroxide gives rise to the iron oxyhydroxide. This reaction can be explained by the next equation:

$$7Fe(OH)_2 + Fe^{2+} + 2Cl^- + \frac{1}{2}O_2 + (2n+1)H_2O \longrightarrow 2[3Fe(OH)_2.Fe(OH)_2Cl.nH_2O] \tag{3}$$

The product of reaction (3) is appointed Green Rust 1 (GR1) [25]. This GR1 is oxidized to form γ-FeOOH, which reacts with $Co(OH)_2$ to form $Co(OH)_2.2FeOOH$

complex. This product was annealed to form cobalt ferrite with cubic spinel phase by removing hydroxide content and complete crystallization:

$$Co(OH)_2.2FeOOH \longrightarrow CoFe_2O_4 + 2H_2O \tag{4}$$

3.2. Structure analysis.

The powder XRD patterns of $CoFe_2O_4$ nanoparticles prepared at different annealing temperature (T_{an} = 773 , 973, 1023, 1073 and 1223 K) are shown in Fig 1. The major peaks are well indexed to the crystallographic planes of spinel ferrite the (220), (222), (400), (422), (511) and (440), with 100% intensity at $2\theta \approx 35.5°$ attributed to (311) reflection plane. As examples the Rietveld

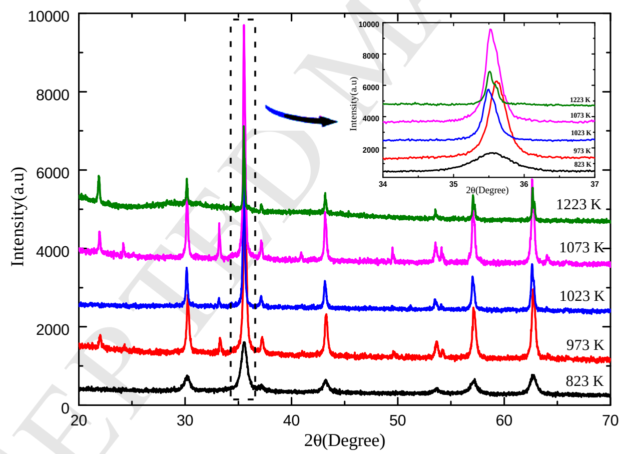

Figure 1: XRD pattern of the $CoFe_2O_4$ annealed samples at 773 , 973, 1023, 1073 and 1223 K during 6 h.

refinement results of XRD pattern of $CoFe_2O_4$ samples annealed at 773 , 1023 and 1223 K are presented in Fig 2. This analysis allows us to identify the impurity and quantify the percentage of each phase. The R_B and χ_2 factors, the lattice parameters, the density and the percentage of each phase are given in Table 1. The refinement performed confirmed the presence of a main phase ($\sim$

85-100 wt%) corresponding to $CoFe_2O_4$ typical of the cubic spinel structure with a $Fd\bar{3}m$ space group and the lattice parameter in the range from 8.3789(4) to 8.3890(2)$\mathring{A}$. Obtained values for lattice parameters a are in agreement with that reported in literatures for cobalt ferrite (a = 8.93 $\mathring{A}$) compounds [26]. However, the rietveld refinement showed the coexistence of two secondary phases where their percentage varies with the annealing temperature. These two phases are β-Fe_2O_3 with space group $R\bar{3}c$ ($\sim$ 1.5-6.3 wt%)and CoO_2 with space group $P\bar{3}m1$ ($\sim$ 3.3-10.2 wt%).

The average crystallite size (D) of each sample was determined from the full width at half maximum ($FWHM$) of most intense peaks of reflection (311) using Debye Scherrer's [27] formula:

$$D = \frac{k\lambda}{\beta cos(\theta)} \tag{5}$$

where λ is the wavelength of $Cu(K_\alpha)$, β is the full width at half maximum ($FWHM$), θ is the Braggs diffraction angle and k is the Scheerers constant (0.90). Herein $\beta = (\beta_M^2$ - $\beta_S^2)$, β_M is the full width at half maximum ($FWHM$) of the most intense peak (311) and β_S is the standard instrumental broadening (0.0480°) [28]. The lattice parameter a which defines the size of unit cell was determined by Rietveld refinement. Fig 3 shows the dependence of crystallite size and lattice parameters as a function of the annealing temperature. The increase of the annealing temperature of the samples is accompanied by an increase in crystallite size. However, and as seen from Fig 3, the increase of the annealing temperature does not affect the lattice parameters.

The crystallite sizes of $CoFe_2O_4$, β-Fe_2O_3 and CoO_2 phases were determined from $CoFe_2O_4$-(311), β-Fe_2O_3-(222) and CoO_2-(001) peak widths, by using Scherrer's formula. This parameter varies from 30 to 178 nm when annealing temperature increases from 773 to 1073 K during 6 h. Furthermore, the Scherrer equation can only be applied for sizes smaller than 1000-2000 $\mathring{A}$ or 100-200 nm [29]. So we can't determine the crystallite size for the sample annealing at 1223 K. However, the increase of β-Fe_2O_3 and CoO_2 content is accompanied by an overall increase in their crystallite sizes and in $CoFe_2O_4$ one.

Table 1: Structural results of $CoFe_2O_4$ samples, R_B and χ^2 factors from Rietveld fit, a is the lattice parameter, D is the crystallite size and ρ_{XRD} is the density value. The sample relate respectively to $CoFe_2O_4$ nanoparticles annealed at 773, 973, 1023, 1073 and 1223 K during 6 h.

Sample	Phase	%	R_B	χ^2	$a(\AA)$	$D(nm)$	D_{SEM}	ρ_{XRD} $(g.cm^{-3})$
773 K	$CoFe_2O_4$	100	2.03	1.22	8.3789(4)	30	35-40	5.29
973 K	$CoFe_2O_4$	93.82	2.22	1.24	8.3890(2)	51	55-60	5.27
	β-Fe_2O_3	2.85	9.62	1.24	5.0389(3)	59		10.51
	CoO_2	3.33	9.02	1.24	4.6889(5)	25		11.07
1023 K	$CoFe_2O_4$	98.49	2.18	1.08	8.3841(5)	120	150-160	5.28
	β-Fe_2O_3	1.51	11.5	1.08	5.0345(1)	27		10.54
1073 K	$CoFe_2O_4$	85.79	1.86	1.35	8.3885(1)	178	185-190	5.28
	β-Fe_2O_3	6.30	8.39	1.35	5.0388(2)	106		10.52
	CoO_2	7.91	9.16	1.35	4.6852(4)	57		10.96
1223 K	$CoFe_2O_4$	89.77	9.79	1.57	8.3824(3)		240-250	5.29
	CoO_2	10.23	12.1	1.57	4.6944(4)	115		11.05

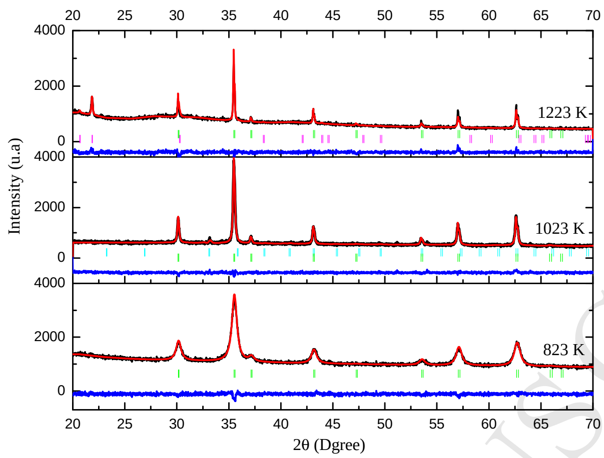

Figure 2: Rietveld analysis for X-ray diffraction pattern of $CoFe_2O_4$ nanoparticles annealed at 773 K, 1023 K and 1223 K (above), Vertical bars represent the positions of the Bragg reflections; the row marks correspond to the $CoFe_2O_4$ and β-Fe_2O_3 type phase. The observed-calculated difference is depicted at the bottom of the figure.

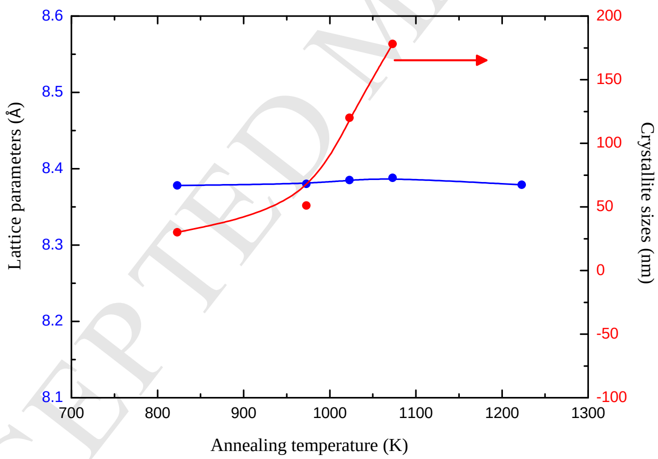

Figure 3: The relationship between the crystallite sizes (D) and lattice parameters and the annealing temperature.

3.3. Morphology structure.

The external morphology of the $CoFe_2O_4$ nanoparticles annealed at 773 K, 1023 K and 1223 K has been visualized by the scanning electron microscopy (SEM). SEM photographs of the growth of ferrite nanoparticles for different temperatures of annealing are shown in Fig 4. It is noted that the particles are spherical in shape and slightly agglomerated. This agglomeration can be attributed to magnetic interaction arising among ferrite nanoparticles. The particle size (DT) calculated from SEM is less than the crystal size estimated from XRD. The SEM images indicate the increase in particle size with increase of the annealing temperature. The cobalt ferrite nanoparticles annealed at a lower annealing temperature were spherical and in the size range of 35-40 nm at 773 K. Further, spherical and elongated big particles were observed at high annealing temperatures. The cobalt ferrite nanoparticles annealed at high annealing temperatures were in the size range of 150-160 nm and 240-250 nm at 1023 K and 1223 K, respectively.

3.4. Magnetic properties.

In order to obtain good extrinsic properties, we present in the following the magnetic measurements on samples annealed at different temperatures. At each annealing temperature, a measure M-H is performed. Fig 5 shows the hysteresis loops at 10 K (bottom) and 300 K (top), for the samples annealed at 773 , 973, 1023, 1073, and 1223 K. These figures confirm the ferrimagnetic behavior at room temperature (300 K) and low temperature (10 K). At 300 K, it is noted that the sample annealed at 1023 K is magnetically harder than the other four samples. Indeed, the coercive field is of 1.58 kOe for this sample against the values of less than 0.61 kOe for the other annealed samples. The high value of the coercive field is higher compared with in the literature of the cobalt ferrites synthesized by Co-precipitation [26, 30] but remains close to that obtained by the sol-gel [31]. The weak magnetic coercive field for these samples is explained by the low grain size as in literature [32], they showed that H_c varies linearly with the inverse of the size until a critical size. Also we note that the remanent magnetization increases up to the 1023 K annealed sample and decreases beyond that. Indeed, the remanent magnetization is of 31.85 $emu.g^{-1}$ for the hard magnetic sample against values below 23 emu.g^{-1} for the softest magnetic samples. The magnetization curves MH obtained at

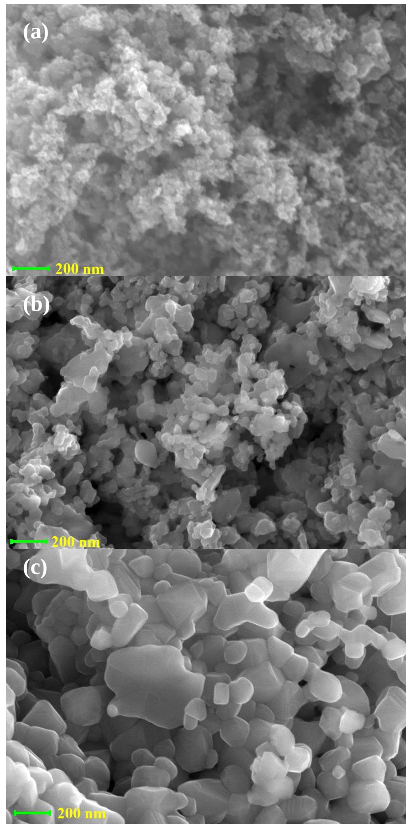

Figure 4: Scanning Electron Microscopy (SEM) images of cobalt ferrite nanoparticles annealed at (a) 773 K, (b) 1023 K and (c) 1223 K.

10 K are represented in Fig 5 (bottom) for all samples. It shows that at 10 K the coercive field is higher than its counterpart at ambient temperature. We note higher values up to 16 kOe for samples annealed between 773 and 1023 K and two to three times lower values for the other two samples. The remanent magnetization is higher for the two samples annealed at 1023 and 1223 K. They are 66.7 and 64.6 emu.g^{-1} respectively. The double hysteresis observed, at 10 K, can be explained by the intrinsic coupling of two magnetic phases soft and hard.

To get insight into the effect of annealing on the magnetic properties, we

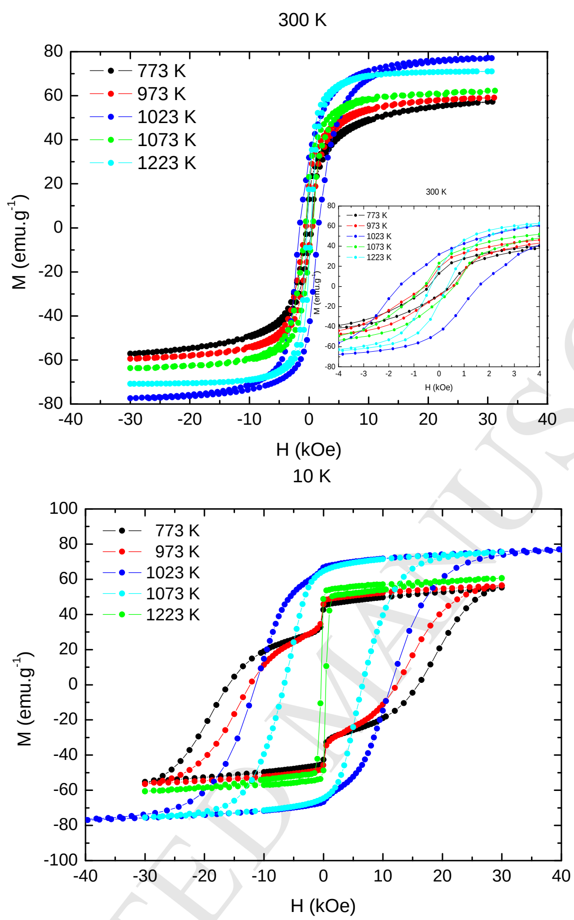

Figure 5: Hysteresis loops of Co-ferrite annealed at 773, 973, 1023, 1073, and 1223 K for 6h min, measured at 10K (bottom) and 300K (top).

have tried to evaluate the magnetic anisotropy MA constant. For that purpose, we used Néels law of approach to saturation [33]:

$$M(H) = M_s \left(1 - \frac{b}{H^2}\right) + \chi_0 H \tag{6}$$

with

$$b = \frac{8}{105}\left(\frac{K_L}{M_s}\right)^2 \tag{7}$$

where H is the applied magnetic field in (T), Ms is the saturation magnetization in $(emu.g^{-1})$, and b is a constant which is a function of K_L the local anisotropy,

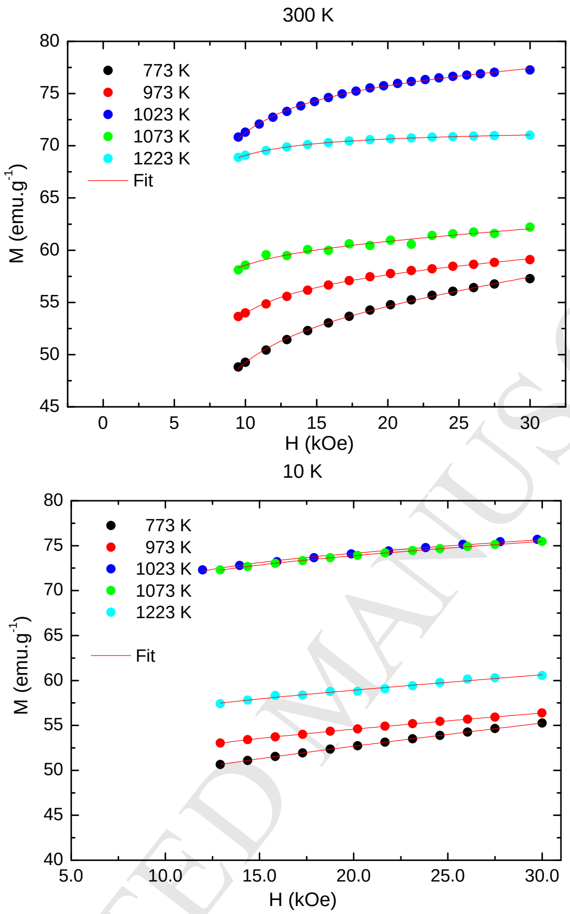

Figure 6: Magnetization curve at 300 K of the cobalt ferrite annealed at 773, 973, 1023, 1073, and 1223 K for 6h min (top) and magnetization curve at 10 K (bottom).

M_s and the symmetry.

The magnetization curves for all samples are found to fit well equation (6), as shown in Fig 6. The values of M_s, and b obtained from the fitting at 10 K and 300 K were used to determine K_L using (7). Values of the parameters obtained this way are shown in Table 2. We find that the local anisotropy at room temperature is of 0.19 $\times 10^6$ $erg.cm^{-3}$ (close to the literature[6]) for all annealed samples except for the hardest magnetic sample where the value is equal to 0.35 $\times 10^6$ $erg.cm^{-3}$.

Table 2: The magnetic data of $CoFe_2O_4$ nanoparticles annealed at 773 , 973, 1023, 1073 and 1223 K during 6 h.

	300 K				10 K			
Sample	H_c(kOe)	K_L (erg.cm^{-3})	M_s (emu.g^{-1})	M_r/M_s	H_c (kOe)	K_L (erg.cm^{-3})	M_s $(emu.g^{-1})$	M_r/M_s
773 K	0.41	2.09×10^5	51.19	0.25	15.94	0.77×10^5	47.95	0.89
973 K	0.55	2.08×10^5	56.39	0.33	12.30	0.90×10^5	51.55	0.89
1023 K	1.58	3.47×10^5	74.85	0.43	11.37	2.49×10^5	72.38	0.92
1073 K	0.61	1.87×10^5	59.32	0.25	6.58	1.38×10^5	71.69	0.90
1223 K	0.33	2.05×10^5	70.87	0.39	0.41	0.45×10^5	55.97	0.87

At room temperature, the saturation magnetization of the hard magnetic sample is 74.85 $emu.g^{-1}$ increasing by 46% compared to the soft magnetic sample annealed at 773 K, $M_s = 51.19$ $emu.g^{-1}$. Moreover, we point out that the ratio M_r/M_s is the highest for the sample annealed at 1023 K. The ratio is 0.43 against the values between 0.25 and 0.39 for the others samples. This may be due to the presence of an antiferromagnetic second phase (β-Fe_2O_3) in the sample annealed at 1023 K (see Table 2) [34]. At low temperature (10 K), the value of magnetization saturation is approximately equal to 71 $emu.g^{-1}$ for both samples which are annealed at 773 K and 1223 K and below 59 $emu.g^{-1}$ for the other samples. On the other hand, the ratio M_r/M_s is greater than 0.8 with the highest value being 0.92 for the sample annealed at 1023 K. This confirms the magnetic hardness of this sample.

Fig 7 shows the B-BH at 10 K (bottom) and 300 K (top) for the samples annealed at 773, 973, 1023, 1073, and 1223 K. The Maximum energy product $(BH)_{Max}$ at room temperature is 0.5 MGOe for the hard magnetic sample (annealed at 1023 K) against the values below at 0.1 MGOe for the softer magnetic samples. This was confirmed by the low temperature measurement, at 10 K, since there is a square hysteresis loop for the sample annealed at 1023 and 1223 K with the ratio M_r/M_s being almost equal to 1 with a slight recess showing the presence of the antiferromagnetic second phase. The coercive field are 6.6 and 11.3 kOe for these samples respectively. This is confirmed by the values of $(BH)_{Max}$ at 10 K wich are 3.9 and 4.1 MGOe for the hards magnetics samples annealed at 1023 and 1223 K respectively.

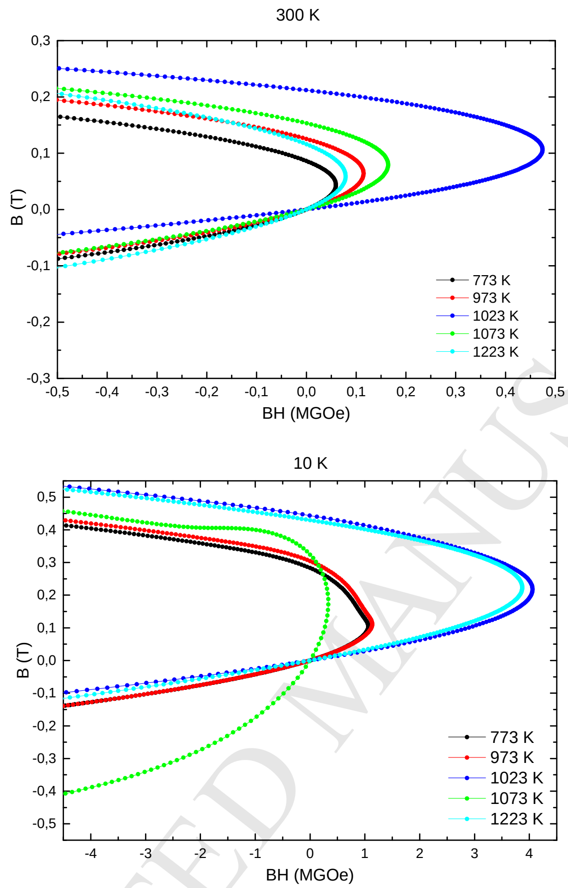

Figure 7: Variation of B as a function (BH) for the annealing samples.

4. Conclusions

This study deals with the synthesis of Cobalt ferrite nanoparticles synthesis by co-precipitation method and annealed at 773, 973, 1023, 1073 and 1223 K. The Rietveld refinement of the structure confirms the presence of a main phase of $CoFe_2O_4$ as well as the secondary phases of β-Fe_2O_3 and CoO_2 respectively. SEM study show that the ferromagnetic nanoparticles are of high quality and the grain sizes increase with increasing in annealing temperatures. The effect of annealing temperature on the magnetic properties and crystallite size of the samples is investigated in order to have suitable magnetic properties and greatly expanding the range of applications. The magnetic results at room temperature show that β-Fe_2O_3 phase allowed us to obtain high coercivity of 1.58 kOe and note that the ratio $M_r/M_s = 0.43$ is the highest for the sample annealed at 1023 K. Regarding the measurements at 10 K, the samples annealed at 1023 and 1223 K manifest high saturation magnetization, a square hysteresis loop and high coercivity which is suitable for fabrication of permanent magnets with $(BH)_{Max}$ equal to 4.1 MGOe. In conclusion, these nanoparticles can be used for high density magnetic recording at room temperature or as permanent magnet at low temperature.

5. Acknowledgements

This work is mainly supported by the CNRS and the Ministére de l'Enseignement Supérieur, de la Recherche Scientifique (Tunisia).

6. References

[1] A. K. Gupta, M. Gupta, Synthesis and surface engineering of iron oxide nanoparticles for biomedical applications, Biomaterials 26 (18) (2005) 3995 – 4021. doi:http://dx.doi.org/10.1016/j.biomaterials.2004.10.012.
URL http://www.sciencedirect.com/science/article/pii/S0142961204009317

[2] X.-H. Huang, Z.-H. Chen, Cofe2o4 nanoparticles hosted in silica xerogels, Scripta Materialia 54 (2) (2006) 169 – 173. doi:http://dx.doi.org/10.1016/j.scriptamat.2005.09.043.
URL http://www.sciencedirect.com/science/article/pii/S1359646205006032

[3] C. C. Berry, A. S. G. Curtis, Functionalisation of magnetic nanoparticles for applications in biomedicine, Journal of Physics D: Applied Physics 36 (13)

(2003) R198.
URL http://stacks.iop.org/0022-3727/36/i=13/a=203

[4] Y. I. Kim, D. Kim, C. S. Lee, Synthesis and characterization of cofe2o4 magnetic nanoparticles prepared by temperature-controlled coprecipitation method, Physica B: Condensed Matter 337 (14) (2003) 42 – 51. doi:http://dx.doi.org/10.1016/S0921-4526(03)00322-3.
URL http://www.sciencedirect.com/science/article/pii/S0921452603003223

[5] D. Kim, Y. Zhang, W. Voit, K. Rao, M. Muhammed, Synthesis and characterization of surfactant-coated superparamagnetic monodispersed iron oxide nanoparticles, Journal of Magnetism and Magnetic Materials 225 (12) (2001) 30 – 36, proceedings of the Third International Conference on Scientific and Clinical Applications of Magnetic Carriers. doi:http://dx.doi.org/10.1016/S0304-8853(00)01224-5.
URL http://www.sciencedirect.com/science/article/pii/S0304885300012245

[6] K. Zehani, R. Bez, A. Boutahar, E. Hlil, H. Lassri, J. Moscovici, N. Mliki, L. Bessais, Structural, magnetic, and electronic properties of high moment feco nanoparticles, Journal of Alloys and Compounds 591 (2014) 58 – 64. doi:http://dx.doi.org/10.1016/j.jallcom.2013.11.208.
URL http://www.sciencedirect.com/science/article/pii/S0925838813029502

[7] A. K. Giri, K. Pellerin, W. Pongsaksawad, M. Sorescu, S. A. Majetich, Effect of light on the magnetic properties of cobalt ferrite nanoparticles, IEEE Transactions on Magnetics 36 (5) (2000) 3029–3031. doi:10.1109/20.908666.

[8] A. K. Giri, E. M. Kirkpatrick, P. Moongkhamklang, S. A. Majetich, V. G. Harris, Photomagnetism and structure in cobalt ferrite nanoparticles, Applied Physics Letters 80 (13) (2002) 2341–2343.

doi:http://dx.doi.org/10.1063/1.1464661.
URL http://scitation.aip.org/content/aip/journal/apl/80/13/10.1063/1.1464661

[9] F. Zhang, S. Kantake, Y. Kitamoto, M. Abe, Spin-spray ferrite-plated co ferrite films with high coercivity for perpendicular magnetic recording media, IEEE Transactions on Magnetics 35 (5) (1999) 2751–2753. doi:10.1109/20.800974.

[10] V. Pillai, D. Shah, Synthesis of high-coercivity cobalt ferrite particles using water-in-oil microemulsions, Journal of Magnetism and Magnetic Materials 163 (12) (1996) 243 – 248. doi:http://dx.doi.org/10.1016/S0304-8853(96)00280-6.
URL http://www.sciencedirect.com/science/article/pii/S0304885396002806

[11] S. Mitra, K. Mandal, S. Sinha, P. M. G. Nambissan, S. Kumar, Size and temperature dependent cationic redistribution in nife 2 o 4 (sio 2) nanocomposites: positron annihilation and mssbauer studies, Journal of Physics D: Applied Physics 39 (19) (2006) 4228.
URL http://stacks.iop.org/0022-3727/39/i=19/a=016

[12] J. Zhou, J. Ma, C. Sun, L. Xie, Z. Zhao, H. Tian, Y. Wang, J. Tao, X. Zhu, Low-temperature synthesis of nife2o4 by a hydrothermal method, Journal of the American Ceramic Society 88 (12) (2005) 3535–3537. doi:10.1111/j.1551-2916.2005.00629.x.
URL http://dx.doi.org/10.1111/j.1551-2916.2005.00629.x

[13] P. E. Meskin, V. K. Ivanov, A. E. Barantchikov, B. R. Churagulov, Y. D. Tretyakov, Ultrasonically assisted hydrothermal synthesis of nanocrystalline zro2, tio2, nife2o4 and ni0.5zn0.5fe2o4 powders, Ultrasonics Sonochemistry 13 (1) (2006) 47 – 53. doi:http://dx.doi.org/10.1016/j.ultsonch.2004.12.002.

URL http://www.sciencedirect.com/science/article/pii/S1350417705000039

[14] S. Li, V. T. John, C. O'Connor, V. Harris, E. Carpenter, Cobalt-ferrite nanoparticles: Structure, cation distributions, and magnetic properties, Journal of Applied Physics 87 (9) (2000) 6223–6225. doi:http://dx.doi.org/10.1063/1.372661.
URL http://scitation.aip.org/content/aip/journal/jap/87/9/10.1063/1.372661

[15] S. Prasad, N. Gajbhiye, Magnetic studies of nanosized nickel ferrite particles synthesized by the citrate precursor technique, Journal of Alloys and Compounds 265 (12) (1998) 87 – 92. doi:http://dx.doi.org/10.1016/S0925-8388(97)00431-3.
URL http://www.sciencedirect.com/science/article/pii/S0925838897004313

[16] R. Panda, J. Shih, T. Chin, Magnetic properties of nano-crystalline gd- or pr-substituted cofe2o4 synthesized by the citrate precursor technique, Journal of Magnetism and Magnetic Materials 257 (1) (2003) 79 – 86. doi:http://dx.doi.org/10.1016/S0304-8853(02)01036-3.
URL http://www.sciencedirect.com/science/article/pii/S0304885302010363

[17] S. Sartale, C. Lokhande, Electrochemical synthesis of nanocrystalline cofe2o4 thin films and their characterization, Ceramics International 28 (5) (2002) 467 – 477. doi:http://dx.doi.org/10.1016/S0272-8842(01)00119-5.
URL http://www.sciencedirect.com/science/article/pii/S0272884201001195

[18] C.-H. Yan, Z.-G. Xu, F.-X. Cheng, Z.-M. Wang, L.-D. Sun, C.-S. Liao, J.-T. Jia, Nanophased cofe2o4 prepared by combustion method, Solid State Communications 111 (5) (1999) 287 – 291.

doi:http://dx.doi.org/10.1016/S0038-1098(99)00119-2.
URL http://www.sciencedirect.com/science/article/pii/S0038109899001192

[19] M. Godinho, M. Catarino, M. da Silva Pereira, M. Mendona, F. Costa, Effect of the partial replacement of fe by ni and/or mn on the electrocatalytic activity for oxygen evolution of the cofe2o4 spinel oxide electrode, Electrochimica Acta 47 (27) (2002) 4307 – 4314. doi:http://dx.doi.org/10.1016/S0013-4686(02)00434-6.
URL http://www.sciencedirect.com/science/article/pii/S0013468602004346

[20] J. Ding, P. McCormick, R. Street, Formation of spinel mn-ferrite during mechanical alloying, Journal of Magnetism and Magnetic Materials 171 (3) (1997) 309 – 314. doi:http://dx.doi.org/10.1016/S0304-8853(97)00093-0.
URL http://www.sciencedirect.com/science/article/pii/S0304885397000930

[21] J. Ding, T. Reynolds, W. F. Miao, P. G. McCormick, R. Street, High magnetic performance in mechanically alloyed co-substituted fe3o4, Applied Physics Letters 65 (24) (1994) 3135–3136. doi:http://dx.doi.org/10.1063/1.112459.
URL http://scitation.aip.org/content/aip/journal/apl/65/24/10.1063/1.112459

[22] Y. Shi, J. Ding, H. Yin, Cofe2o4 nanoparticles prepared by the mechanochemical method, Journal of Alloys and Compounds 308 (12) (2000) 290 – 295. doi:http://dx.doi.org/10.1016/S0925-8388(00)00921-X.
URL http://www.sciencedirect.com/science/article/pii/S092583880000921X

[23] H. M. Rietveld, A profile refinement method for nuclear and magnetic

structures, Journal of Applied Crystallography 2 (2) (1969) 65–71. doi:10.1107/S0021889869006558.
URL http://dx.doi.org/10.1107/S0021889869006558

[24] J. Rodriguez-Carvajal, M. T. Fernandez-Diaz, J. L. Martinez, Neutron diffraction study on structural and magnetic properties of la 2 nio 4, Journal of Physics: Condensed Matter 3 (19) (1991) 3215.
URL http://stacks.iop.org/0953-8984/3/i=19/a=002

[25] P. Refait, S. Drissi, J. Pytkiewicz, J.-M. Gnin, The anionic species competition in iron aqueous corrosion: Role of various green rust compounds, Corrosion Science 39 (9) (1997) 1699 – 1710. doi:http://dx.doi.org/10.1016/S0010-938X(97)00076-0.
URL http://www.sciencedirect.com/science/article/pii/S0010938X97000760

[26] M. Houshiar, F. Zebhi, Z. J. Razi, A. Alidoust, Z. Askari, Synthesis of cobalt ferrite (cofe2o4) nanoparticles using combustion, coprecipitation, and precipitation methods: A comparison study of size, structural, and magnetic properties, Journal of Magnetism and Magnetic Materials 371 (2014) 43 – 48. doi:http://dx.doi.org/10.1016/j.jmmm.2014.06.059.
URL http://www.sciencedirect.com/science/article/pii/S0304885314005812

[27] J. Sun, Z. Wang, Y. Wang, Y. Zhu, T. Shen, L. Pang, K. Wei, F. Li, Synthesis of the nanocrystalline cofe2o4 ferrite thin films by a novel solgel method using glucose as an additional agent, Materials Science and Engineering: B 177 (2) (2012) 269 – 273. doi:http://dx.doi.org/10.1016/j.mseb.2011.12.017.
URL http://www.sciencedirect.com/science/article/pii/S0921510711005320

[28] Y. Kseoglu, F. Alan, M. Tan, R. Yilgin, M. ztrk, Low temperature hydrothermal synthesis and characterization of mn doped cobalt fer-

rite nanoparticles, Ceramics International 38 (5) (2012) 3625 – 3634. doi:http://dx.doi.org/10.1016/j.ceramint.2012.01.001.
URL http://www.sciencedirect.com/science/article/pii/S027288421200003X

[29] G. N. Holzwarth U, The scherrer equation versus the 'debye-scherrer equation, Nat Nano 6 (2011) 534–534.

[30] S. Gyergyek, D. Makovec, A. Kodre, I. Arčon, M. Jagodič, M. Drofenik, Influence of synthesis method on structural and magnetic properties of cobalt ferrite nanoparticles, Journal of Nanoparticle Research 12 (4) (2010) 1263–1273. doi:10.1007/s11051-009-9833-5.
URL http://dx.doi.org/10.1007/s11051-009-9833-5

[31] M. B. Ali, K. E. Maalam, H. E. Moussaoui, O. Mounkachi, M. Hamedoun, R. Masrour, E. Hlil, A. Benyoussef, Effect of zinc concentration on the structural and magnetic properties of mixed cozn ferrites nanoparticles synthesized by sol/gel method, Journal of Magnetism and Magnetic Materials 398 (2016) 20 – 25. doi:http://dx.doi.org/10.1016/j.jmmm.2015.08.097.
URL http://www.sciencedirect.com/science/article/pii/S0304885315305205

[32] R. Masrour, M. Hamedoun, A. Benyoussef, The magnetic properties of diluted cofe 2 o 4 nanomaterials, Chinese Physics B 21 (4) (2012) 047501.
URL http://stacks.iop.org/1674-1056/21/i=4/a=047501

[33] L. Néel, La loi d'approche en a: H et une nouvelle thorie de la duret magntique, J. Phys. Radium 9 (5) (1948) 184–192. doi:10.1051/jphysrad:0194800905018400.
URL http://dx.doi.org/10.1051/jphysrad:0194800905018400

[34] S. Sakurai, A. Namai, K. Hashimoto, S. ichi Ohkoshi, First observation of phase transformation of all four fe2o3 phases, Journal of the American

Chemical Society 131 (51) (2009) 18299–18303, pMID: 19938830. doi: 10.1021/ja9046069.
URL http://dx.doi.org/10.1021/ja9046069

Highlights :

- The nanoparticles cobalt ferrite was synthesized in co-precipitation process.
- Subsequently, the cobalt ferrite is annealed under air at different temperature between 773 and 1223 K.
- Their Structural, morphological, and magnetic properties have been presented.
- The samples annealed at 1023 K for 6h possess a coercive field of 1.5 and 11.4 kOe at room temperature and low temperature respectively.
- The sample annealed at 1023 K for 6 h exhibits the best $(BH)_{max}$ (BH_{max} = 0.5 MGOe at 300 K and 3.9 MGOe at 10 K).